Photoredox Reactions

International Edition: DOI: 10.1002/anie.201603530
German Edition: DOI: 10.1002/ange.201603530

Picomole-Scale Real-Time Photoreaction Screening: Discovery of the Visible-Light-Promoted Dehydrogenation of Tetrahydroquinolines under Ambient Conditions

*Suming Chen[+], Qiongqiong Wan[+], and Abraham K. Badu-Tawiah**

Abstract: *The identification of new photocatalytic pathways expands our knowledge of chemical reactivity and enables new environmentally friendly synthetic applications. However, the development of miniaturized screening procedures/platforms to expedite the discovery of photochemical reactions remains challenging. Herein, we describe a picomole-scale, real-time photoreaction screening platform in which a handheld laser source is coupled with nano-electrospray ionization mass spectrometry. By using this method, we discovered an accelerated dehydrogenation pathway for the conversion of tetrahydroquinolines into the corresponding quinolines. This transformation is readily promoted by an off-the-shelf [Ru(bpy)$_3$]Cl$_2$·6 H$_2$O complex in air at ambient temperature in direct sunlight, or with the aid of an energy-saving lamp. Moreover, radical cations and trans-dihydride intermediates captured by the screening platform provided direct evidence for the mechanism of the photoredox reaction.*

Recently, photochemical synthesis driven by safe solar photons has attracted significant attention owing to a global drive toward renewable, clean, and sustainable energy technologies.[1] Therefore, the discovery of new photocatalytic reactions, which expand synthetic chemistry through the utilization of solar energy, has become increasingly important. Screening approaches[2] have become the mainstay of discovery processes to identify new chemical reactions and have increased the efficiency of reaction development. The use of microchannel reactors[3] is one of the most common approaches and provides an effective means of photoreaction screening. However, such studies usually require at least milligram (micromole) quantities of substrate per reaction, which may be a prohibitively large amount in preliminary reaction screening. Furthermore, the extra analytical procedures needed to evaluate the reaction add further complications and provide limited insight into the reaction mechanism. The miniaturization of reactions to enable the use of reagents in nanomole-scale quantities or less, combined with real-time product detection that offers access to fleeting intermediates, is a potential solution to this problem. However, no such approach has been developed for sub-nanomole-scale photoreaction screening.

Catalytic dehydrogenation is one of the most common reactions for the large-scale manufacturing of commodity chemicals.[4] In particular, the catalytic dehydrogenation of tetrahydroquinolines to quinolines has attracted broad interest.[5] Much attention has been focused on the development of mild reaction conditions and efficient catalytic systems for high-yielding reactions. However, most reaction systems involving transition-metal-based catalysts require long reaction times and moderately high temperatures (typically $>100\,^{\circ}C$). Recently, a [Ru(phd)$_3$]$^{2+}$/Co(salophen) cocatalyst system (phd = 1,10-phenanthroline-5,6-dione) was synthesized efficiently and found to promote the dehydrogenation of some tetrahydroquinolines to quinolines in relatively short reaction times (5–6 h) under ambient conditions.[5d] Photocatalytic reactions are seldom reported for this transformation. Mesoporous graphite carbon nitride was recently developed that was capable of the catalytic dehydrogenation of 1,2,3,4-tetrahydroquinoline to quinoline upon illumination with visible light for 4.5 h at $100\,^{\circ}C$.[5e] The development of a mild catalytic system involving readily available catalysts for this dehydrogenation reaction is still desirable and will facilitate chemical synthesis.

In the present study, we aimed to 1) develop a picomolar photoreaction screening platform to support rapid photoreaction discovery, 2) study the underlying mechanism of discovered reaction pathways, and 3) use this mechanism to develop the reaction into a preparative-scale synthetic method. By coupling a portable laser source with nano-electrospray ionization (nESI) mass spectrometry (MS), we were able to establish the first MS-based[6] picomole-scale real-time photoreaction screening platform. This platform can be used for the direct and rapid screening of chemical transformations, and results are available within seconds of reaction initiation. With this screening platform, we discovered an effective photocatalytic pathway involving the dehydrogenation of 1,2,3,4-tetrahydroquinolines to the corresponding quinolines. Surprisingly, the reaction was catalyzed by the common visible-light-harvesting complex [Ru(bpy)$_3$]Cl$_2$ (bpy = 2,2′-bipyridine) under ambient conditions. The corresponding scaled up dehydrogenation reactions afforded the desired products in excellent yield in 2–4 h at ambient temperature, either under irradiation with an energy-saving lamp or by exposure to sunlight. Both sets of conditions show significant advantages over current methods. When combined with tandem MS, this method enabled the characterization of the structure of the ruthenium complexes. Furthermore, this real-time MS method[7] enabled the capture

[*] Dr. S. M. Chen,[+] Dr. Q. Q. Wan,[+] Prof. Dr. A. K. Badu-Tawiah
Department of Chemistry and Biochemistry
The Ohio State University
Columbus, OH 43210 (USA)
E-mail: badu-tawiah.1@osu.edu

[+] These authors contributed equally.

Supporting information for this article can be found under: http://dx.doi.org/10.1002/anie.201603530.

of radical cations and *trans*-dihydride intermediates involved in the photoredox reaction and provided direct evidence for the reaction mechanism.

The photoreaction screening platform is as shown in Figure 1a (see Scheme S1 in the Supporting Information for a photograph of the setup). We used a readily available handheld laser source (laser pointer), which allowed the generation of high lighting power density and coherent blue visible light. This light was directed toward miniscule volumes of reaction mixture contained in the transparent glass capillary of the nESI emitter. Charged microdroplets containing reactants/products were generated when a direct current (DC) voltage of 1.0 kV was applied to the solution. Synchronized application of the laser source and the DC voltage enabled analysis of the photoreaction in real time. Furthermore, the MS detection method allowed both the qualitative (on the basis of the MS/MS fragmentation pattern) and quantitative assessment (by measuring ion intensity) of reaction progress.

To validate the utility of this method, we first analyzed the photocatalyzed dehydrogenation (removal of two hydrogen atoms) from the linear secondary amines **1a** and **1b** with $[Ru(bpy)_3]Cl_2 \cdot 6H_2O$ (**5**; Figure 1b). In the absence of light, nESI MS analysis of a mixture of dibenzylamine (**1a**; MW = 197) and **5** (5 mol%) produced the protonated derivative of **1a** at *m*/*z* 198 (Figure 1c). However, in the presence of laser light, a high abundance of ions corresponding to the expected dehydrogenation product *N*-benzylidenebenzylamine (*m*/*z* 196) was observed within seconds (Figure 1d); this peak corresponds to a loss of 2 Da as compared to that of reactant at *m*/*z* 198. The product yield was calculated (see Figure S1 in the Supporting Information for the correction of ionization efficiencies) as 60% (real time; see Table S1), as compared to a 6% yield for the control experiment (100 μM reactant and 5 μM catalyst **5** in CH_3CN under ambient conditions without laser irradiation). Interestingly, the photoredox reaction ceased immediately after the photon irradiation was turned off. Application of the DC voltage continuously, while the laser source was turned off, enabled products to be removed and ensured that the small glass reactor tip was filled with fresh reagent (see Figure S2). This favorable recovery allowed different experimental conditions to be continuously monitored in a single capillary. For example, while the DC voltage was turned off, the reaction mixture could be continuously exposed to light. Results showed an increased yield of 83% when irradiation was continued for 1 min (see Figure S3c), as opposed to 60% for real-time analysis. A further increase in the light-exposure time to 2 min led to a yield of 92% (see Figure S3d). Similar results were recorded for the dehydrogenation reaction of *N*-phenylbenzylamine (**1b**; MW = 183) to generate *N*-benzylideneaniline (*m*/*z* 182; see Figure S4). These results indicate that by using the new MS-based photoreaction screening approach, the reactivity of reactants can be judged in seconds, in contrast to traditional photoreaction experiments that require a reaction time of several hours. The high efficiency of the current platform may be associated with confinement effects typical of microreactor systems[8] and the high irradiance of the laser source.

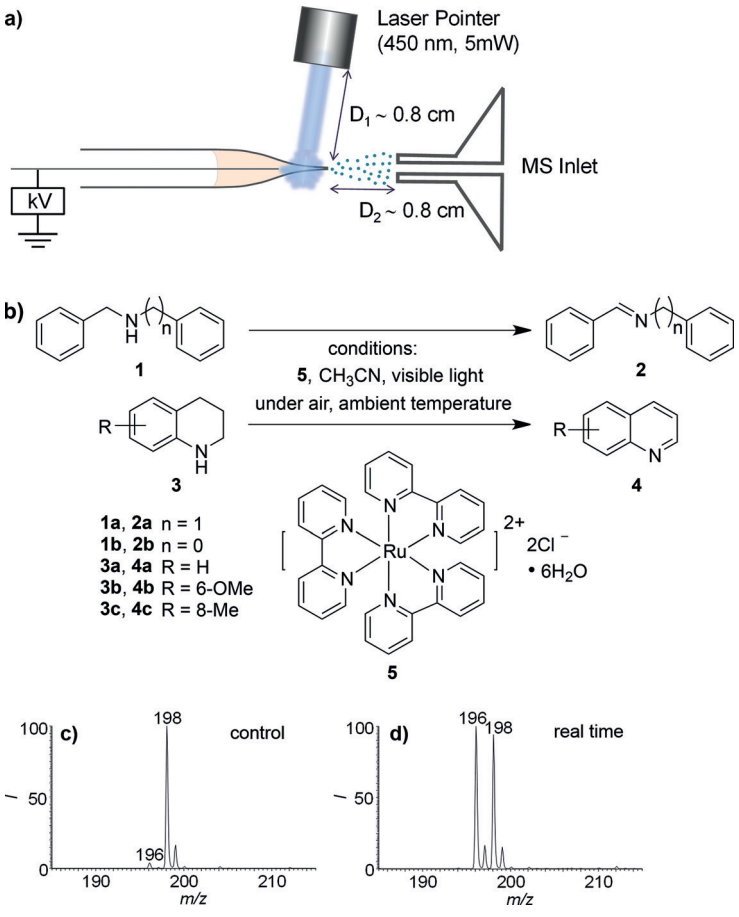

Figure 1. a) Schematic illustration of the real-time photoreaction screening platform. The electrospray voltage is 1.0 kV. b) Photocatalyzed dehydrogenation of 1,2,3,4-tetrahydroquinolines and linear secondary amines. c,d) This approach was used to monitor the progress of the photocatalytic conversion of **1a** (*m*/*z* 198, 100 μM) in the presence of **5** (5 μM) in CH_3CN in positive-ion mode without (c, control) or with laser irradiation (d, real time).

The high photocatalytic activity of off-the-shelf photocatalyst **5** towards the dehydrogenation of linear secondary amines was surprising. We further tested its efficiency on the more difficult transformation of removing four hydrogen atoms from 1,2,3,4-tetrahydroquinolines; to the best of our knowledge, this transformation has not been reported before. We selected 1,2,3,4-tetrahydroquinoline (**3a**), 6-methoxy-1,2,3,4-tetrahydroquinoline (**3b**), and 8-methyl-1,2,3,4-tetrahydroquinoline (**3c**) as model compounds and evaluated their susceptibility towards the ruthenium-based dehydrogenation reaction. The catalyst **5** was sensitive and effective during the photocatalytic conversion of **3** into quinolines **4** (Figure 2). Protonated species derived from **3a** (*m*/*z* 134) were observed in the absence of light (Figure 2a). Only trace amounts of the intermediate (3,4-dihydroquinoline, *m*/*z* 132) and product **4a** (*m*/*z* 130) were detected. Upon application of the laser, the intensity of the peaks for the intermediate at *m*/*z* 132

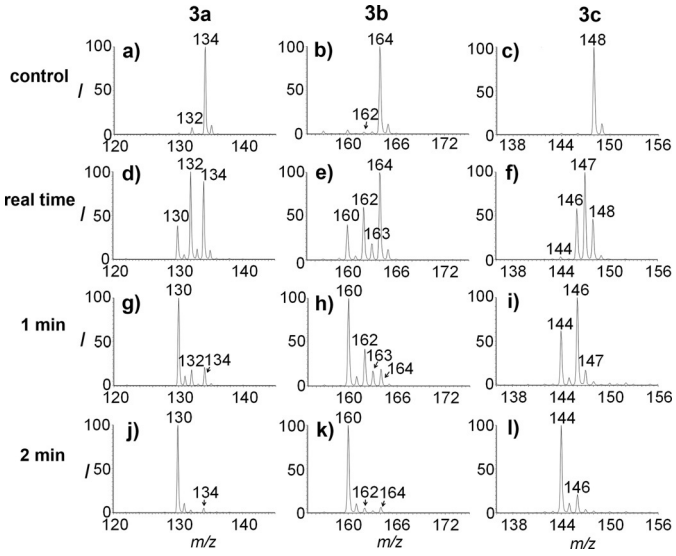

Figure 2. Use of the photoreaction screening platform to monitor the photocatalytic conversion of 1,2,3,4-tetrahydroquinolines **3** (**3a** at *m*/*z* 134, **3b** at *m*/*z* 164, and **3c** at *m*/*z* 148) into quinolines **4** (**4a** at *m*/*z* 130, **4b** at *m*/*z* 160, and **4c** at *m*/*z* 144) in positive-ion mode. Control: MS spectra for **3** (100 μM) and **5** (5 μM) in CH_3CN without laser irradiation. Real time: MS spectra recorded after the simultaneous application of DC spray voltage and laser irradiation. The third and fourth horizontal rows show mass spectra recorded after continuous irradiation of the reaction mixture for 1 and 2 min, respectively. *I* is the relative abundance of detected ions.

and final product **4a** at *m*/*z* 130 significantly increased in real time (Figure 2d), with the corresponding relative ion intensity (see photoreaction screening method and the calculation in the Supporting Information); the intensity increased from 7 and 1% (control; see Table S1) to 44 and 17% (real time; see Table S1), respectively. The relative distribution of intermediate and product ions had changed after continuous light exposure for just 1 min (Figure 2g), during which the amount of intermediate (*m*/*z* 132) decreased to 13% (see Table S1), thus enabling the conversion into **4a** (72%; see Table S1). Laser exposure for 2 min resulted in the depletion of the intermediate (2%; see Table S1), thus generating quinoline with 93% relative ion intensity (Figure 2j). Similar reaction progression and product distributions were observed for the photocatalyzed dehydrogenation of **3b** (Figure 2b,e,h,k) and **3c** (Figure 2c,f,i,l). Under the same conditions, however, no products were observed in the absence of catalyst **5** (see Figures S5 and S6), thus demonstrating the key role of this photocatalyst. Furthermore, the correlated increase in relative ion intensity with irradiation time implies that the light-triggered catalytic effect in the capillary is the predominant process, as compared with contributing effects from the droplet environment.[6b] No evident dehydrogenation products were observed when the rapidly moving charged droplets were illuminated (see Figure S7). Interestingly, radical cations formed from the initial interaction of the amine with the excited Ru complex were detected for reactants **3b** and **3c** at *m*/*z* 163 (Figure 2e) and *m*/*z* 147 (Figure 2f), respectively. The capture of the radical cations in our method provides key information regarding the mechanism (as discussed later) of this ruthenium-based photocatalyzed dehydrogenation reaction.

To investigate whether the dehydrogenation reaction occurring in the screening platform is unique to the electrochemical environment of the electrospray process, we developed a non-electrical gas-driven spray MS analytical apparatus (see Figure S8). All intermediates, including radical cations (*m*/*z* 132, 162, 163, 146, and 147), from the conversion of **3a**, **3b**, and **3c** could also be observed by using this non-electrical apparatus under laser irradiation (see Figure S9). This result indicates that the production of these intermediates, especially radical cations, can be ascribed to a photocatalytic and not an electrochemical process. In contrast, no conversion of these reactants was observed in the nano-electrospray capillary, even at an increased voltage of 4 kV, with the laser light source turned off (see Figure S10). Moreover, the photocatalytic dehydrogenation of linear secondary amines (see Figure S11) and 1,2,3,4-tetrahydroquinolines (see Figure S12) proceeded with ease in an off-line experiment in centrifuge tubes under laser irradiation. This observation further demonstrates that these reactions do not rely on the electrical environment of the nESI MS detection method. These results collectively suggested the possibility of extending the screened small-scale reactions to a larger-scale synthesis.

We began a detailed investigation of the new ruthenium-based photoreaction by performing the reaction in bulk solution under the ambient loading conditions of photocatalyst **5**; however, the laser light source used in the screening platform was replaced with a common energy-saving lamp (23 W) and sunlight. The results of these bulk-phase reactions are in agreement with those obtained from the photoreaction screening platform. The linear amines **1a** and **1b** were converted into the corresponding imines in high yields of 81 and 96%, respectively, when irradiated with the lamp for 1.5 h (Table 1). In the case of **3a**, the fully dehydrogenated quinoline **4a** was formed in 86% yield under sunlight for 2 h at 35 °C and in 73% yield under lamp light for 2 h at 25 °C. Furthermore, **3b** was transformed into 6-methoxyquinoline (**4b**) in 46% yield when exposed to

Table 1: Scaled-up dehydrogenation of **1** and **3** by the Ru complex.[a]

Compound	Light	Catalyst loading [mol%]	*t* [h]	Yield[b] [%]
1a	lamp	5	1.5	81 (**2b**)
1b	lamp	5	1.5	96 (**2a**)
3a	sun light	5	2	86 (**4a**)
3a	lamp	5	2	73 (**4a**)
3b	sun light	1	2	46 (**4b**)
3b	lamp	1	2	40 (**4b**)
3b	lamp	3	2	71 (**4b**)
3c	sun light	5	2	53 (**4c**)
3c	lamp	5	4	65 (**4c**)

[a] Reaction conditions: A solution (3 mL) of **1** or **3** (10 mM) and **5** was exposed to a 23 W energy-saving lamp at 25 °C or sun light (outdoor temperature: 35 °C). [b] The yield was determined by ^{1}H NMR analysis (400 MHz) of the crude reaction mixture with (1*Z*,5*Z*)-cycloocta-1,5-diene as an internal standard.

sunlight and in 40% yield under the lamp with a catalyst loading of only 1%. Among the substrates examined, only sterically demanding **3c** required a longer reaction time of 4 h, after which a 65% yield of 8-methyl-quinoline **4c** was obtained under lamp light. This is due to the inefficient conversion from the imine intermediate. The production of **4a** under sun light was also monitored by ^{1}H NMR spectroscopy with the standard reagents **3a** and **4a** as controls (see Figure S13). We found that **3a** was fully dehydrogenated to give **4a** under ambient conditions (see details of the characterization of the reaction products in Figures S14–S22). We believe this finding is significant because the catalytic approach described herein is a simple and effective method for obtaining quinolines under visible light with an off-the-shelf catalyst under ambient conditions. This MS-based screening approach for structural analysis was also used to characterize the occurrence of ruthenium-based complexes (see Figures S23–S28 and related discussion in the Supporting Information).

The above experimental evidence and the strong dependence of this photocatalyzed dehydrogenation on oxygen (see Figure S29–S33) led us to propose an aerobic photoredox oxidation mechanism (Scheme 1). First, the active $[Ru(bpy)_3]^{2+}$ species is converted into the excited-state complex $[Ru^*(bpy)_3]^{2+}$ upon irradiation with visible light. Subsequently, single-electron transfer from the 1,2,3,4-tetrahydroquinoline **3** to the excited-state complex $[Ru^*(bpy)_3]^{2+}$ takes place. This process generates $[Ru(bpy)]^+$ and the radical-cation intermediate **A**, which were detected by both electrospray-based analysis and the non-electrical gas-driven spray method at m/z 163 (Figure 2e; see also Figure S8e) and m/z 147 (Figure 2f; see also Figure S9f) for the 6-methoxy- and 8-methyl-1,2,3,4-tetrahydroquinoline reactants, respectively. O_2 is known to be involved in one-electron transfer from $[Ru(bpy)]^+$ to form the superoxide radical anion ($O_2^{\bullet-}$).[9] We believe $O_2^{\bullet-}$ is the main active species in the visible-light-mediated ruthenium-based dehydrogenation reaction. $O_2^{\bullet-}$ can abstract two hydrogen atoms from the radical cation to form a dihydroquinoline product **B** and H_2O_2.[10] The presence of H_2O_2 in the reaction mixture was detected in a titration reaction with KI (see Figure S34).[11] Tautomerization of the dihydroquinoline intermediate **B** into **C** (Scheme 1; these intermediates are almost energetically equal)[12] allows the generation of the final quinoline product through a second dehydrogenation step.

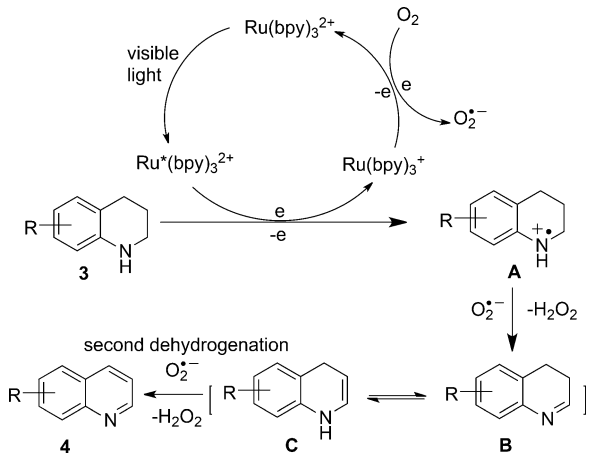

Scheme 1. Proposed reaction mechanism.

In conclusion, by coupling a handheld laser source with nESI MS, we have established a picomole-scale real-time photoreaction screening platform. The platform exhibits high efficiency and rapid photoreaction screening capabilities. A new chemical transformation involving the conversion of tetrahydroquinolines into quinolines with $[Ru(bpy)_3]Cl_2{\cdot}6H_2O$ was discovered, and the corresponding radical-cation intermediates were captured on the photoreaction platform in real time. More importantly, the larger-scale reactions confirm that the new dehydrogenation pathway can proceed under ambient conditions with visible-light sources, such as sunlight. We believe that this platform may find application in the discovery of other novel photoreactions.

Acknowledgements

This research was supported by start-up funds of the Ohio State University.

Keywords: dehydrogenation · mass spectrometry · reaction screening · quinolines · visible light

How to cite: *Angew. Chem. Int. Ed.* **2016**, *55*, 9345–9349
Angew. Chem. **2016**, *128*, 9491–9495

[1] a) T. P. Yoon, M. A. Ischay, J. Du, *Nat. Chem.* **2010**, *2*, 527–532; b) T. P. Yoon, C. R. J. Stephenson, *Adv. Synth. Catal.* **2014**, *356*, 2739; c) K. Zeitler, *Angew. Chem. Int. Ed.* **2009**, *48*, 9785–9789; *Angew. Chem.* **2009**, *121*, 9969–9974.

[2] a) K. D. Collins, T. Gensch, F. Glorius, *Nat. Chem.* **2014**, *6*, 859–871; b) D. W. Robbins, J. F. Hartwig, *Science* **2011**, *333*, 1423–1427; c) A. B. Santanilla, E. L. Regalado, T. Pereira, M. Shevlin, K. Bateman, L. C. Campeau, J. Schneeweis, S. Berritt, Z. C. Shi, P. Nantermet, Y. Liu, R. Helmy, C. J. Welch, P. Vachal, I. W. Davies, T. Cernak, S. D. Dreher, *Science* **2015**, *347*, 49–53; d) T. J. Montavon, J. Li, J. R. Cabrera-Pardo, M. Mrksich, S. A. Kozmin, *Nat. Chem.* **2012**, *4*, 45–51; e) J. R. Cabrera-Pardo, D. I. Chai, S. Liu, M. Mrksich, S. A. Kozmin, *Nat. Chem.* **2013**, *5*, 423–427.

[3] a) E. E. Coyle, M. Oelgemöller, *Photochem. Photobiol. Sci.* **2008**, *7*, 1313–1322; b) M. Oelgemöller, O. Shvydkiv, *Molecules* **2011**, *16*, 7522–7550; c) T. Rodrigues, P. Schneider, G. Schneider, *Angew. Chem. Int. Ed.* **2014**, *53*, 5750–5758; *Angew. Chem.* **2014**, *126*, 5858–5866.

[4] a) K. Yamaguchi, N. Mizuno, *Chem. Eur. J.* **2003**, *9*, 4353–4361; b) K. Suzuki, F. Tang, Y. Kikukawa, K. Yamaguchi, N. Mizuno, *Angew. Chem. Int. Ed.* **2014**, *53*, 5356–5360; *Angew. Chem.* **2014**, *126*, 5460–5464.

[5] a) S. Chakraborty, W. W. Brennessel, W. D. Jones, *J. Am. Chem. Soc.* **2014**, *136*, 8564–8567; b) K. Fujita, Y. Tanaka, M. Kobayashi, R. Yamaguchi, *J. Am. Chem. Soc.* **2014**, *136*, 4829–4832; c) S. I. Murahashi, Y. Okano, H. Sato, T. Nakae, N. Komiya, *Synlett* **2007**, 1675–1678; d) A. E. Wendlandt, S. S. Stahl, *J. Am. Chem. Soc.* **2014**, *136*, 11910–11913; e) F. Su, S. C. Mathew, L. Mohlmann, M. Antonietti, X. Wang, S. Blechert, *Angew. Chem. Int. Ed.* **2011**, *50*, 657–660; *Angew. Chem.* **2011**, *123*, 683–686;

f) J. Wu, D. Talwar, S. Johnston, M. Yan, J. Xiao, *Angew. Chem. Int. Ed.* **2013**, *52*, 6983 – 6987; *Angew. Chem.* **2013**, *125*, 7121 – 7125; g) R. Yamaguchi, C. Ikeda, Y. Takahashi, K. Fujita, *J. Am. Chem. Soc.* **2009**, *131*, 8410 – 8412.

[6] a) F. Bächle, J. Duschmale, C. Ebner, A. Pfaltz, H. Wennemers, *Angew. Chem. Int. Ed.* **2013**, *52*, 12619 – 12623; *Angew. Chem.* **2013**, *125*, 12851 – 12855; b) A. K. Badu-Tawiah, A. Li, F. P. M. Jjunju, R. G. Cooks, *Angew. Chem. Int. Ed.* **2012**, *51*, 9417 – 9421; *Angew. Chem.* **2012**, *124*, 9551 – 9555; c) S. Chen, C. Xiong, H. Liu, Q. Wan, J. Hou, Q. He, A. K. Badu-Tawiah, Z. Nie, *Nat. Nanotechnol.* **2015**, *10*, 176 – 182; d) X. Ma, Y. Xia, *Angew. Chem. Int. Ed.* **2014**, *53*, 2592 – 2596; *Angew. Chem.* **2014**, *126*, 2630 – 2634.

[7] a) T. A. Brown, H. Chen, R. N. Zare, *Angew. Chem. Int. Ed.* **2015**, *54*, 11183 – 11185; *Angew. Chem.* **2015**, *127*, 11335 – 11337; b) T. A. Brown, H. Chen, R. N. Zare, *J. Am. Chem. Soc.* **2015**, *137*, 7274 – 7277.

[8] a) T. Dwars, E. Paetzold, G. Oehme, *Angew. Chem. Int. Ed.* **2005**, *44*, 7174 – 7199; *Angew. Chem.* **2005**, *117*, 7338 – 7364; b) H. Song, D. L. Chen, R. F. Ismagilov, *Angew. Chem. Int. Ed.* **2006**, *45*, 7336 – 7356; *Angew. Chem.* **2006**, *118*, 7494 – 7516.

[9] J. M. R. Narayanam, C. R. J. Stephenson, *Chem. Soc. Rev.* **2011**, *40*, 102 – 113.

[10] Z. Q. Wang, M. Hu, X. C. Huang, L. B. Gong, Y. X. Xie, J. H. Li, *J. Org. Chem.* **2012**, *77*, 8705 – 8711.

[11] L. Huang, J. Zhao, S. Guo, C. Zhang, J. Ma, *J. Org. Chem.* **2013**, *78*, 5627 – 5637.

[12] H. Li, J. Jiang, G. Lu, F. Huang, Z. X. Wang, *Organometallics* **2011**, *30*, 3131 – 3141.

Received: April 11, 2016
Revised: May 4, 2016
Published online: June 20, 2016

